Zigzags, Railroads, and Knots in Fullerenes

M. Deza and M. Dutour

CNRS and LIGA, École Normale Supérieure, 45 rue d'Ulm, 75230 Paris, France

P. W. Fowler*

Department of Chemistry, University of Exeter, Stocker Road, Exeter EX4 4QD, U.K.

Received January 29, 2004

Two connections between fullerene structures and alternating knots are established. Knots may appear in two ways: from *zigzags*, i.e., circuits (possibly self-intersecting) of edges running alternately left and right at successive vertices, and from *railroads*, i.e., circuits (possibly self-intersecting) of edge-sharing hexagonal faces, such that the shared edges occur in opposite pairs. A z-knot fullerene has only a single zigzag, doubly covering all edges: in the range investigated ($n \leq 74$) examples are found for C_{34} and all C_n with $n \geq 38$, all chiral, belonging to groups C_1, C_2, C_3, D_3, or D_5. An r-knot fullerene has a railroad corresponding to the projection of a nontrivial knot: examples are found for C_{52} (trefoil), C_{54} (figure-of-eight or Flemish knot), and, with isolated pentagons, at C_{96}, C_{104}, C_{108}, C_{112}, C_{114}. Statistics on the occurrence of z-knots and of z-vectors of various kinds, z-uniform, z-transitive, and z-balanced, are presented for trivalent polyhedra, general fullerenes, and isolated-pentagon fullerenes, along with examples with self-intersecting railroads and r-knots. In a subset of z-knot fullerenes, so-called minimal knots, the unique zigzag defines a specific Kekulé structure in which double bonds lie on lines of longitude and single bonds on lines of latitude of the approximate sphere defined by the polyhedron vertices.

1. INTRODUCTION

Two structural vectors which play important roles in the classification of polyhedra are the vertex-degree vector $v = \{v_3, v_4, ...\}$ and the face-size vector $p = \{p_3, p_4, ...\}$, where v_r and p_r are the numbers of vertices of degree r and faces of size r, respectively. Euler's theorem gives necessary conditions[1] for realizability of a given v, p pair (the Eberhard problem[2]). Entries in v and p satisfy

$$\sum_r (6-r)v_r \geq 12; \quad \sum_r (6-r)p_r \geq 12; \quad \sum_r (4-r)(v_r + p_r) = 8 \quad (1)$$

Sufficient conditions are known for various classes of polyhedra.[2−4] Alternative formulations of the third requirement are sometimes seen.[5]

Some polyhedra of particular interest in carbon chemistry are the fullerenes, C_n, which are trivalent ($v_3 = n$, $v_r = 0$, otherwise), have only pentagonal and hexagonal faces ($p_5 = 12$, $p_6 = n/2 - 10$, $p_r = 0$, otherwise), and are mathematically realizable for all $n = 20 + 2p_6$ with the exception of $p_6 = 1$.[4] Isomeric fullerenes share v- and p-vectors but differ in the arrangement of their 12 pentagonal faces. A number of fullerene polyhedra with vertex counts in the range of 60 to ∼100, all with disjoint pentagonal faces (isolated-pentagon fullerenes, in the chemical terminology), have been characterized as all-carbon molecular cages. When n is of moderate size, a useful notation, taken up in IUPAC nomenclature, is to label isomers of the C_n fullerene n:m where m is the place of the isomer in the lexicographical order of spiral codes for the set of general or isolated-pentagon fullerenes.[6]

The present paper is concerned with a third structural property, the *zigzag* vector z, which carries information about the *edges* of the polyhedron and makes finer distinctions within sets of isomeric polyhedra. This vector can provide an overwhelming amount of detail for general polyhedra, and we intend here only to identify some basic notions and use them as a framework for the study of the zigzag vectors of fullerenes. In particular, we discuss two connections between *fullerene* zigzag vectors and *knots*.

Knots appear for fullerenes in at least two ways. First, in what may be considered the simplest case of zigzag structure, when a given fullerene has only a *single* zigzag circuit, the Schlegel diagram of the fullerene yields a *projection of a knot*. It will be shown that some (minimal) knots then define a unique Kekulé structure (perfect matching) on the corresponding fullerene, thus establishing an unexpected connection between mathematical knots and the electronic structure of fullerenes as chemical entities.

Second, among fullerenes with *more than one* zigzag circuit, some exhibit a pairing of zigzag circuits in which two parallel (i.e. nonintersecting, concentric) circuits of edges bound a circuit of hexagonal faces, or *"simple railroad"*. The concept can be extended to include self-intersecting railroads. Simple and (doubly) self-intersecting railroads are associated with projections of alternating knots defined by the adjacencies of the hexagonal faces. Simple railroads give a point of departure for cylindrical expansion of fullerenes and a formal route to construction of capped nanotubes.

* Corresponding author phone: 44 1392 263 466; fax: 44 1392 263 434; e-mail: P.W. Fowler@ex.ac.uk.

10.1021/ci049955h CCC: $27.50
Published on Web 05/12/2004

We are aware of a previous connection made between fullerenes and knots: Jablan[7] gives a construction by which a Kekulé structure on a fullerene or other trivalent graph can be associated to a planar 4-valent graph with digons on double bonds and hence to a projection of an alternating knot; our method is different in that the knots arise from the structure of the fullerene itself.

The zigzag and railroad structures, even when restricted to the fullerene class of polyhedra, still give rise to a huge diversity of cases, and in the present paper we make only an initial exploration of these two limiting situations, using computer methods to catalog some of the different possibilities. Computer programs were written, in GAP[8] to deal with the identification and characterization of zigzags and related structures in trivalent polyhedra, taking point-group symmetry into account. Zigzag structures were computed systematically for the trivalent polyhedra ($n \leq 24$), the general fullerenes ($n \leq 74$), isolated-pentagon fullerenes ($n \leq 120$), and icosahedral fullerenes ($n \leq 2000$). The required input information for the computations is the adjacency list and embedding of the graph on the sphere. For the trivalent graphs, this was obtained using the plantri program,[9] and for the fullerenes it was generated from their face spirals[6] and in larger cases from general expressions for the spirals of the icosahedral fullerenes.[10] Material obtained from these computer searches is reported in tables and figures throughout the paper, as the various concepts are introduced and discussed.

The plan of the paper is as follows. Zigzag circuits and the associated concept of the *z*-vector are introduced in section 2. Properties of the *z*-vector are explored in section 3 and discussed for the set of icosahedral fullerenes in section 4. *z*-knot fullerenes are defined in section 5 as the fullerenes with exactly one zigzag circuit. Symmetries of *z*-knot fullerenes are discussed in section 6, and section 7 goes on to define the relationship between minimal *z*-knot fullerenes and a specific Kekulé structure. Section 8 defines railroads of hexagons and shows that these too can lead to an association with knots, giving rise to the definition of *r*-knot fullerenes. Section 9 concludes the paper with an outlook for the wider application of zigzags to description of the structural motifs that appear in chemistry.

2. ZIGZAG VECTORS

In this paper we consider only plane graphs, i.e., graphs that are embedded without crossings in the plane, although in fact the conceptual framework and many of the results extend to graphs embedded in other orientable and nonorientable surfaces. The *z-vector* describes the structure of the zigzag circuits of edges of a graph embedded in a surface. A *zigzag circuit* (*zigzag*, for short) is a cyclically ordered set of edges in which each consecutive pair has one vertex in common and successive edges are chosen by taking alternately leftmost and rightmost edges emanating from the common vertex. For a planar, three-connected graph embedded on the sphere, i.e., for a polyhedron, any two, but not any three, consecutive edges of the circuits belong to the same face. This latter statement is taken as the defining property of Petrie circuits by Coxeter.[11] Circuits of this type are variously called *Petrie*,[11] *left-right*,[12] *geodesic*,[4] or *zigzag* circuits. Since for each edge there are two possible directions for extension of a zigzag circuit, and since any two adjacent edges bounding a face define a zigzag, the set of zigzag circuits gives an exact *double cover* of the edges: any edge appears either twice in the same zigzag or once each in two different zigzags.

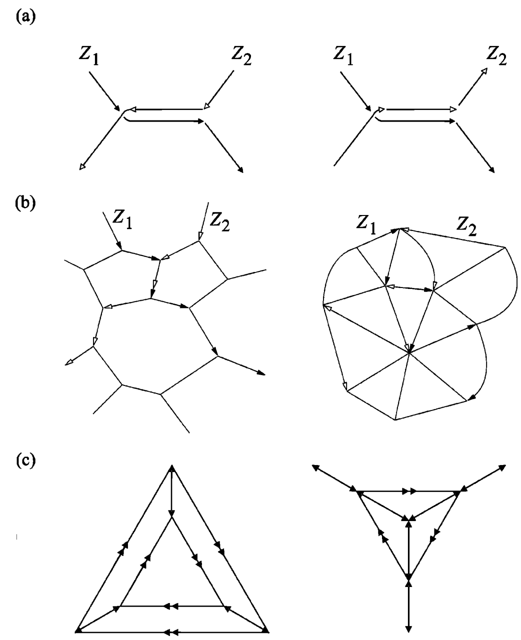

Figure 1. Self-intersection in zigzags. (a) Definition of edge types. Arrows with solid (Z_1) and empty (Z_2) heads represent portions of the same zigzag circuit $Z = Z_1...Z_2$. If they run in opposite senses along an edge where they intersect, that edge is of type I, if in the same sense, the edge is of type II. (b) Relation between edge types in dual maps. Z_1, Z_2, $Z_2...Z_2$ in the map (right) are converted to Z'_1 and Z'_2, $Z'_1...Z'_2$ in the dual (left). In the original map, the edge on which intersection takes place is of type II, but in the dual its image is of type I. The length of $Z_1...Z_2$ is not changed; a zigzag vector entry l_{e_1,e_2} is replaced by l_{e_2,e_1} in the dual. (c) Zigzag vectors of a pair of dual polyhedra: the trigonal prism and the trigonal bipyramid. Each has a single zigzag circuit, covering all edges exactly twice. A specific orientation is indicated on the Schlegel diagram for each polyhedron by the arrow markings. Edges marked with an arrowhead at each end are traversed once in each direction, those marked with a double arrowhead are traversed twice in the same direction. The *z*-vectors are, respectively, $(18_{3,6})$ and $(18_{6,3})$.

An explicit notation for the *z*-vector must take into account the possibility that a given zigzag circuit may intersect with itself. If the circuit is equipped with an orientation, the arrows on an edge where self-intersection (if any) takes place run in either the opposite (*type* I) or the same sense (*type* II) (see Figure 1(a)).[4] (In Shank's classification,[12] these two types correspond respectively to cocycle and cycle character of left-right circuits.) The pair of numbers e_1, e_2 that count the edges of types I and II is the *signature* of the zigzag. Simple (i.e. nonself-intersecting) zigzags have signature (0, 0).

Thus, the *z*-vector is a vector that lists, in increasing order of length, the lengths of zigzags, with their signature appearing as a subscript and the number of zigzags of that length (the multiplicity) as a superscript. Simple zigzags are listed with the (0, 0) signatures suppressed and are collected at the beginning of the vector, separated from the self-intersecting zigzags (if any) by a semicolon. The multiplicity superscript is suppressed when equal to 1.

Note that a polyhedron P and its dual $P^\star$ are related by interchanging *v*- and *p*-vectors and have the same distribution

Table 1. Zigzag Structure of the Fullerenes C_n with $n \leq 40$ Vertices[a]

n	z-vectors				
20	(10^{6})				
24	$(12; 60_{12,12})$				
26	$(12^{3}; 42_{0,9})$				
28	$(12; 32_{0,4}, 40_{0,8})$	(12^{7})			
30	$(10^{2}; 70_{15,10})$	$(22_{0,1}, 68_{6,18})$	$(12^{3}; 54_{2,13})$		
32	$(14; 82_{10,24})$	$(14^{2}; 34^{2}_{0,4})$	$(14^{3}; 54_{0,12})$	$(12, 14; 70_{10,14})$	$(12^{3}; 30_{0,3}, 30_{3,0})$
	$(12; 84_{18,18})$				
34	$(102_{17,34})$	$(12, 14^{3}; 48_{1,8})$	$(12; 30_{0,3}, 60_{7,9})$	$(14^{2}; 74_{5,20})$	$(14^{2}; 74_{7,18})$
	$(30_{0,3}, 72_{12,12})$				
36	$(46_{0,7}, 62_{4,11})$	$(16; 22^{2}_{0,1}, 48_{4,4})$	$(12, 14; 36_{0,4}, 46_{1,7})$	$(12, 14; 82_{19,11})$	$(12, 16; 80_{20,8})$
	$(12; 30^{2}_{0,3}, 36_{0,4})$	$(14; 94_{12,28})$	$(14^{2}; 30_{0,3}, 50_{0,9})$	$(14^{4}; 26^{2}_{0,1})$	$(46_{0,8}, 62_{4,12})$
	$(14^{2}; 30_{0,3}, 50_{0,9})$	$(14^{5}; 38_{0,4})$	$(26^{3}_{0,1}, 30_{0,3})$	$(14^{4}; 26^{2}_{0,1})$	$(12^{2}, 14^{6})$
38	$(16; 98_{12,29})$	$(16^{3}; 22^{3}_{0,1})$	$(12; 102_{20,25})$	$(16; 36_{0,4}, 62_{7,8})$	$(114_{21,36})$
	$(114_{29,28})$	$(14, 16; 84_{11,18})$	$(14; 26_{0,1}, 74_{5,17})$	$(114_{27,30})$	$(114_{19,38})$
	$(14; 38_{0,4}, 62_{2,13})$	$(16; 48_{2,6}, 50_{1,8})$	$(14^{2}; 86_{9,22})$	$(14^{3}; 26_{0,1}, 46_{0,8})$	$(12^{2}, 14^{2}; 62_{1,14})$
	$(14^{6}; 30_{0,3})$	$(14^{4}; 58_{1,12})$			
40	$(10^{3}; 90_{20,10})$	$(34_{0,2}, 86_{18,10})$	$(16; 104_{28,16})$	$(12; 52_{4,5}, 56_{3,8})$	$(12; 24_{0,1}, 84_{15,12})$
	$(16^{2}; 88_{7,23})$	$(24_{0,1}, 96_{12,25})$	$(16^{3}; 22_{0,1}, 50_{1,8})$	$(16; 38_{0,4}, 66_{10,6})$	$(16; 52_{1,8}, 52_{4,5})$
	$(50_{4,4}, 70_{6,12})$	$(16; 104_{20,24})$	$(16; 38_{0,4}, 66_{7,9})$	$(14; 26_{0,1}, 80_{15,10})$	$(16; 104_{22,22})$
	$(14^{2}, 16; 76_{10,12})$	$(14; 106_{16,30})$	$(14; 106_{18,28})$	$(14^{4}, 16; 48_{4,4})$	$(12^{2}; 96_{21,15})$
	$(16; 38_{0,4}, 66_{6,10})$	$(120_{21,39})$	$(38_{0,4}, 82_{6,20})$	$(26_{0,1}, 94_{10,25})$	$(14, 16; 90_{14,18})$
	$(14; 106_{14,32})$	$(26_{0,1}, 94_{10,25})$	$(14^{2}; 26_{0,1}, 66_{2,15})$	$(14^{3}; 78_{6,18})$	$(14^{3}; 78_{6,18})$
	$(14^{2}; 30_{0,3}, 62_{2,13})$	$(12^{2}, 16; 80_{8,16})$	$(12^{2}, 14^{2}; 34^{2}_{1,2})$	$(14^{2}, 16; 76_{9,13})$	$(14^{2}, 16; 76_{8,14})$
	$(14^{3}; 78_{4,20})$	$(14^{4}, 16; 48_{2,6})$	$(14^{2}; 46^{2}_{0,8})$	$(14^{5}; 50_{0,10})$	$(30^{4}_{0,3})$

[a] For vertex count n, z-vectors are listed by isomer, in spiral lexicographic order.[6]

Table 2. Zigzag Structure of All Isolated-Pentagon Fullerenes C_n with $n \leq 84$ Vertices[a]

n	z-vectors				
60	(18^{10})				
70	$(20^{5}; 110_{0,25})$				
72	$(108_{0,24}, 108_{12,12})$				
74	$(20^{9}; 42_{0,3})$				
76	$(20; 56_{0,4}, 152_{8,40})$	$(20^{3}; 42^{4}_{0,3})$			
78	$(18^{2}; 198_{39,42})$	$(38_{0,1}, 196_{22,58})$	$(20^{2}; 64_{0,8}, 130_{4,31})$	$(18^{2}; 198_{39,42})$	$(42_{0,3}, 64^{3}_{0,8})$
80	$(22^{5}; 130_{0,30})$	$(22^{2}; 98^{2}_{0,16})$	$(20, 22^{2}; 86_{2,13}, 90_{5,10})$	$(20^{3}, 22^{3}; 114_{12,12})$	$(42_{0,1}, 90_{5,10}, 108_{6,18})$
	$(20^{2}; 90_{5,10}, 110_{15,10})$	(20^{12})			
82	$(20^{2}, 22^{4}; 118_{7,18})$	$(20, 22^{3}; 160_{15,34})$	$(22^{2}; 202_{23,58})$	$(22^{2}; 202_{25,56})$	$(42^{2}_{0,1}, 162_{17,32})$
	$(20^{2}; 42^{2}_{0,1}, 122_{9,16})$	$(42^{3}_{0,1}, 120_{12,12})$	$(20^{6}; 42^{3}_{0,1})$	$(20^{4}; 42^{2}_{0,1}, 82_{1,8})$	
84	$(24; 72_{0,8}, 78^{2}_{0,9})$	$(94_{0,15}, 158_{12,35})$	$(22^{2}; 46_{0,3}, 162_{8,41})$	$(20; 46^{2}_{0,3}, 140_{8,28})$	$(20; 46^{2}_{0,3}, 140_{12,24})$
	$(22^{4}; 82^{2}_{0,9})$	$(42_{0,1}, 46_{0,3}, 82^{2}_{0,9})$	$(22^{4}; 42_{0,1}, 122_{4,21})$	$(20^{2}, 22^{5}; 102_{4,12})$	$(20^{2}, 22^{4}; 42_{0,1}, 82_{1,8})$
	$(20^{2}, 22^{3}; 42^{2}_{0,1}, 62_{0,4})$	$(20^{2}, 22^{3}; 42^{2}_{0,1}, 62_{0,4})$	$(20^{2}, 22^{2}; 42^{4}_{0,1})$	$(22^{2}; 42^{3}_{0,1}, 82_{0,9})$	$(22^{2}; 42^{3}_{0,1}, 82_{0,9})$
	$(20^{4}, 22^{4}; 42^{2}_{0,1})$	$(20^{4}, 22^{4}; 42^{2}_{0,1})$	$(20^{2}, 22^{2}; 42^{4}_{0,1})$	$(20^{6}, 22^{6})$	$(42^{6}_{0,1})$
	$(20^{2}, 22^{4}; 62^{2}_{0,4})$	$(20^{2}, 22^{2}; 42^{4}_{0,1})$	$(42^{6}_{0,1})$	$(20^{6}, 22^{6})$	

[a] For vertex count n, the z-vectors are listed for all isomers in the spiral lexicographic order.[6]

of *lengths* of zigzags *but* with each signature *reversed* (Figure 1(b)). Figure 1(c) shows this reversal in the simple case of the trigonal prism and its dual, the trigonal bipyramid. Component-wise, $P \leftrightarrow P^{\star}$ is therefore associated with $v_r \leftrightarrow p_r$ and, in the z-vector, $l^{m}_{e1,e2} \leftrightarrow l^{m}_{e2,e1}$. In the present case, the trigonal prism has z-vector $(18_{3,6})$ and the trigonal bipyramid has $(18_{6,3})$.

As examples, the z-vectors of the tetrahedron, cube (and octahedron), and dodecahedron (and icosahedron) are (4^{3}), (6^{4}), and (10^{6}). All have only simple zigzags, and hence there is no need for explicit signatures. On the other hand, any $(2k + 1)$-gonal prism has $z = ((12k + 6)_{2k+1,4k+2})$ with all vertical edges (those that connect top and bottom $(2k + 1)$-gonal faces) being of type I and all horizontal edges (those that belong to top or bottom faces) being of type II. Among the small fullerenes, the unique barrel-like 24-vertex and egg-shaped 26-vertex fullerenes have $z = (12;60_{12,12})$ and $z = (12^{3};42_{0,9})$, respectively.

Table 1 lists all z-vectors for the set of fullerenes with $n \leq 40$ vertices, obtained by explicit computation on the adjacency information generated from their face spirals. Symmetries, spectral data, and illustrations of the three-dimensional forms of these fullerenes, along with lists of the face spirals are available.[6] Table 2 lists z-vectors for the isolated-pentagon fullerenes with $n \leq 84$ vertices, including the experimentally observed isomers of C_{60}, C_{70}, C_{76}, C_{78}, and C_{84}.

These simple census tables already reveal some new information on the discriminatory power of the z-vector. Table 1 gives some data relevant to an observation made by Grünbaum on trivalent polyhedra. He remarks[3] that it is not known whether a knowledge of both the p-vector of face

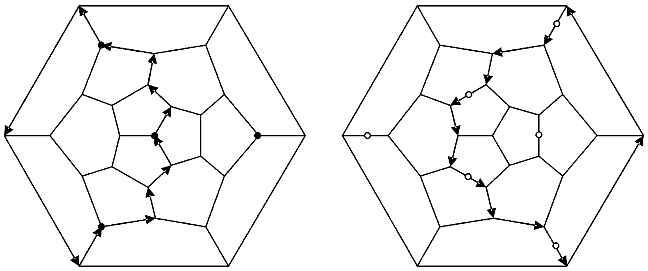

(a) (b)

Figure 2. The smallest fullerene that is *z*-uniform but not *z*-transitive. Schlegel diagrams of the tetrahedral isomer (28:2) are shown marked with nonequivalent zigzag circuits. In maximum T_d symmetry, points at which three pentagonal faces meet form the vertices of a regular tetrahedron (filled circles); the six edge-midpoints of this master tetrahedron are marked with open circles. The zigzag in (a) passes through three vertices of the tetrahedron and belongs to an orbit for four equivalent circuits; the zigzag in (b) passes through four edge-midpoints, leaving out one antipodal pair, and belongs to an orbit of three equivalent circuits. All seven zigzags are simple and of length 12.

sizes and the *z*-vector is sufficient to determine the combinatorial type of a trivalent polyhedron. As the table shows, already for small fullerenes there are pairs of isomers with equal *z*-vectors. Considering only lengths of zigzags, then the C_{34} isomers 34:4 and 34:5, both of C_2 symmetry, each have two simple zigzags of length 14 and one other of length 24. Isomers 36:9 (C_{2v} symmetry) and 36:14 (D_{2h} symmetry) have exact coincidence of *z*-vector lengths and intersection patterns. C_s 36:8 and C_2 36:11 also form such a pair. Table 2 shows that pairs with the same *z*-vector and intersection signature also occur among the isolated-pentagon fullerenes. Isomers 78:1(D_3) and 78:4(D_{3h}) is the smallest such pair; a pair in which all zigzags are simple is 84:19(D_{3d})/84:24-(D_{6h}); a pair in which all zigzags are of the same length and signature is 84:20(T_d)/84:23(D_{2d}). C_{60}, C_{78}:1, and C_{84}:23 are all examples where experimental fullerene isomers share their zigzag structure with a less stable partner.

3. PROPERTIES OF ZIGZAG VECTORS

Given a trivalent polyhedron, we will call it *z-uniform* if all zigzags have the same length and the same signature, i.e., if the *z*-vector has only one component. In general, the zigzags are partitioned into orbits by the action of the symmetry group of the polyhedron, and it is clear that two zigzags may belong to the same orbit only if they have equal length and share the same signature. If there is only *one* orbit of zigzags, the polyhedron is called *z-transitive*. Clearly, *z*-transitivity implies *z*-uniformity. The dodecahedron, with its *z*-vector of (10^6) is *z*-uniform and *z*-transitive; the next two fullerenes, those with 24 and 26 vertices, are neither *z*-uniform nor *z*-transitive; the tetrahedral isomer of the 28-vertex fullerene has *z*-vector (12^7), and so is *z*-uniform, but cannot be *z*-transitive as the group T_d has no orbit of size 7 (its zigzags fall into two orbits (Figure 2)). Table 3 lists *z*-uniform fullerenes with $n \leq 60$ vertices, and Table 4 lists the *z*-uniform isolated-pentagon fullerenes with $n \leq 100$ vertices.

For any zigzag Z, we can define an *intersection vector* Int(Z) which lists the sizes of its intersections with itself and with all other zigzags, with multiplicities, in increasing order of number of common edges. This vector has first entry

Table 3. Zigzag Uniform Fullerenes C_n for $n \leq 60$[a]

isomer n:m	group	orbit size	z-vector length	signature	intersection vector
20:1	I_h	6	10	0,0	$0; 2^5$
28:2	T_d	4, 3	12	0,0	$0; 2^6$
40:40	T_d	4	30	0,3	$3; 8^3$
44:73	T	3	44	0,4	$4; 18^2$
44:83	D_2	2	66	5,10	15; 36
48:84	C_2	2	72	7,9	16; 40
48:188	D_3	3, 3, 3	16	0,0	$0; 2^8$
52:237	C_3	3	52	2,4	$6; 20^2$
52:437	T	3	52	0,8	$8; 18^2$
56:293	C_2	2	84	7,13	20; 44
56:349	C_2	2	84	5,13	18; 48
56:393	C_3	3	56	3,5	$8; 20^2$
60:1193	C_2	2	90	7,13	20; 50
60:1197	D_2	2	90	13,8	21; 48
60:1803	D_3	6,3,1	18	0,0	$0; 2^9$
60:1812	I_h	10	18	0,0	$0; 2^9$

[a] Those with only a single zigzag (*z*-knot fullerenes) are not listed, as they are trivially *z*-uniform.

Table 4. Zigzag Uniform Isolated-Pentagon Fullerenes C_n for $n \leq 100$[a]

isomer n:m	group	orbit size	z-vector length	signature	intersection vector
80:7	I_h	12	20	0, 0	$0^2; 2^{10}$
84:20	T_d	6	42	0, 1	$1; 8^5$
84:23	D_{2d}	4,2	42	0, 1	$1; 8^5$
86:19	D_3	3	86	1, 10	$11; 32^2$
88:34	T	12	22	0, 0	$0; 2^{11}$
92:86	T	6	46	0, 3	$3; 8^5$
94:110	C_3	3	94	2, 13	$15; 32^2$
100:387	C_2	2	150	13, 22	35; 80
100:432	D_2	2	150	17, 16	33; 84
100:438	D_2	2	150	15, 20	35; 80
100:445	D_2	2	150	17, 16	33; 84

[a] As in Table 3, only those cases that are not *z*-knots are listed. *z*-Uniformity implies *z*-transitivity when the number of orbits is one.

$e_1 + e_2$ for the intersection of the zigzag with itself, separated by a semicolon from a series of entries $e_i^{r_i}$ for r_i, the number of zigzags that have e_i edges in common with the subject zigzag. The self-intersection component and its accompanying semicolon is suppressed when the intersection is equal to 0, i.e., for a simple zigzag.

A polyhedron will be called *z-balanced* if all zigzags of each given length and signature have the same intersection vector. Again, all *z*-transitive polyhedra are, by definition, *z*-balanced, as both *z*-uniformity and *z*-balance are relaxations of the notion of *z*-transitivity. The connection between *z*-uniformity and *z*-balance is less clear. In one direction, it is easy to find fullerenes that are *z*-balanced but not *z*-uniform; in the other, so far, however, we have no examples of fullerenes that are *z*-uniform but not *z*-balanced.

The smallest general fullerene that is *not* *z*-balanced has 52 vertices and D_{2d} symmetry (isomer 52:94); its zigzag vector is (16^4;$92_{12,12}$); not all of its four zigzags of length 16 have the same intersection vector.[13] If the *z*-balanced fullerene is required to have only simple zigzags, then the smallest example is a D_{2d} 108-vertex isomer with zigzag vector (24^8, 26^4, 28). It is known from tests performed in the present work on a catalog of the fullerenes with simple zigzags[15] that any *z*-uniform fullerene with only simple zigzags and $n \leq 200$ vertices is also *z*-balanced.

Table 5. Icosahedrally Symmetric z-Uniform Fullerene Isomers C_n for $n \leq 2000$[a]

			z-vector		
n	i, j	N_z	length	signature	intersection vector
20	1, 0	6	10	0, 0	$0; 2^5$
60	1, 1	10	18	0, 0	$0; 2^9$
140	2, 1	15	28	0, 0	$0; 2^{14}$
260	3, 1	10	78	0, 3	$3; 8^9$
380	3, 2	6	190	0, 15	$15; 32^5$
420	4, 1	6	210	5, 10	$15; 36^5$
620	5, 1	6	310	15, 10	$25; 52^5$
740	4, 3	6	370	0, 25	$25; 64^5$
780	5, 2	6	390	0, 25	$25; 68^5$
860	6, 1	10	258	0, 9	$9; 24^3, 28^6$
980	5, 3	10	294	0, 9	$9; 28^3, 32^6$
1140	7, 1	15	228	0, 4	$4; 14^8, 18^6$
1220	5, 4	15	244	0, 4	$4; 14^4, 18^{10}$
1340	7, 2	15	268	0, 8	$8; 18^{14}$
1460	8, 1	10	438	0, 18	$18; 42^3, 46^6$
1580	7, 3	10	474	0, 18	$18; 46^3, 50^6$
1820	6, 5	6	910	0, 70	$70; 154^5$
1820	9, 1	6	910	30, 40	$70; 154^5$
1860	7, 4	6	930	0, 70	$70; 158^5$
1920	8, 3	6	970	10, 70	$80; 162^5$

[a] Only those cases defined by coprime pairs (i, j) are listed, as the zigzag properties of all others can be deduced from the coprime cases, as described in the text. N_z is the number of zigzags.

We note that the intersection of two simple zigzags in a fullerene can be arbitrarily long; it has been shown, for example, that any even number h can be realized as the intersection size of two simple zigzags in a fullerene on $18h - 8$ vertices (Theorem 7.1[13]).

Further to the earlier remarks on discriminatory power, it has been established that two isomeric fullerenes can have the same z-vector entries. Table 3 shows that the similarity between isomers can be even closer: notice the existence of a C_{60} fullerene (60:1803) that is identical in zigzag length, signature, and intersection with the isolated-pentagon icosahedral isomer (60:1812) and differs only in its orbit decomposition;[16] the existence of this pair is a counterexample to an implicit conjecture[3] that for simple polyhedra the p- and z-vectors together define the combinatorial type (i.e. the isomer) and shows that resolution of isomers is not achieved even with full intersection information.

4. ZIGZAG STRUCTURE OF ICOSAHEDRAL FULLERENES

The mathematically simplest fullerenes are the icosahedral family. Molecular graphs for I_h and I fullerenes are all available by the Goldberg-Coxeter construction,[14,17,18] in which two integer parameters specify a net on the triangulation of the plane. The vertex counts of I and I_h fullerenes are

$$n = 20(i^2 + ij + j^2) \qquad (2)$$

with integers $0 \leq j \leq i$, $i > 0$. The fullerene has I_h symmetry whenever $i = j$ or $j = 0$ i.e., when $j(i - j) = 0$, and has I symmetry, otherwise.

The results on z-vectors of the icosahedral fullerenes C_n with $n < 2000$ are listed in Table 5. A number of observations can be drawn from them. First we note that it is sufficient to study only the case where the Goldberg parameters i and j are *coprime*. This is because, by the nature of the construction, the change from i, j to ki, kj changes the zigzag structure in the following way: both the length of the zigzag and the multiplicity with which that length occurs are scaled by k. For example, any I_h fullerene $(i, 0)$ has $z = ((10i)^{6i})$ and any I_h fullerene (i, i) has $z = ((18i)^{10i})$.

It is also observed that all icosahedral fullerenes are z-uniform, but it turns out that icosahedral fullerenes are z-transitive only for the greatest common divisor $k = 1$, and 2 i.e., for (i, j) and $(2i, 2j)$. In general, if the coprime parent (i, j) has $z = (l^t)$, then the derived (ki, kj) has $k/2$ orbits of size $2t$ (when k is even) or $(k - 1)/2$ orbits of size $2t$ and one orbit of size t (when k is odd). The length of the zigzags follows from the fact that the product of length and multiplicity is $3n$. From the computations it is observed that t is one of 6, 10, 15 in all cases—no orbits of size 60 or 120 are found. It has been proved that t always takes one of these three values.[18] For example, the case of C_{80} (I_h) is $(i, j) = (2, 0)$, derived from $(1, 0)$ with $k = 2$. C_{80} (I_h) has 1 orbit of $2 \times 6 = 12$ zigzags, each of length $2 \times 10 = 20$, having signature (0, 0) and intersection vector $(0;2^{10}, 0)$. In the same way, C_{240} (I_h), with $(i, j) = (2, 2)$ derives from C_{60} (I_h) and shows doubling of zigzags in both length and number. There are various regularities in the multiplicities, signatures, and intersection vectors which are revealed on more detailed number-theoretic analysis.[18]

The icosahedral series of fullerenes admits the possibility of isomerism in that the expression for the vertex count, n, may admit multiple solutions (i, j) with $i \leq j$. At $n = 980$, there are two nonisomorphic icosahedral fullerenes; one is chiral and has coprime parameters $(i, j) = (5, 3)$; the other is achiral (7, 0) and hence derives from (1, 0) with $k = 7$. The chiral isomer has 10 zigzags, of length 294 and signature (9, 0) with intersection vector $(9;28^3, 32^6)$ (Table 5); the achiral isomer has 42 zigzags, of length 70, and signature (0, 0) with intersection vector $(0;2^{35}, 0^6)$. At $n = 1820$, there are two nonisomorphic chiral icosahedral fullerenes, both with coprime parameters, represented by $(i, j) = (6, 5)$ and (9, 1), and as Table 5 shows, they have the same number of zigzags (6), the same length of zigzag (910), and the same intersection, each zigzag intersecting 154 times with the 5 others, but the two isomers are distinguished by their signatures (e_1, e_2).

5. A CONNECTION OF ZIGZAG VECTORS WITH KNOTS

Zigzags correspond to *straight-ahead* (or *central*[16]) circuits in the medial graph—circuits that leave each vertex by the edge diametrically opposite to the one by which they entered. Central circuits cover the edges of the medial graph exactly once. The *medial* of an embedded planar graph is a four-valent graph, the vertices of which correspond to the edges of the original, and whose edges connect vertices that correspond to edges sharing a vertex and a face in the original polyhedron; a graph and its dual have therefore the same medial. Any four-valent plane graph can be seen as a projection of an *alternating link*[19−21]—just take a straight-ahead path going alternately under and over at consecutive intersections.

As a single-component link is a *knot*, it is appropriate to call those fullerenes that have only a single zigzag circuit, and hence whose medial is a projection of an alternating

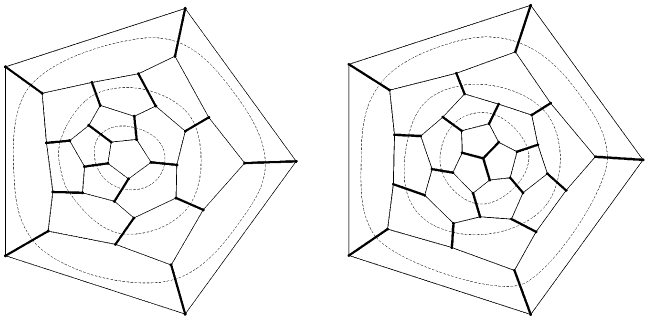

(a) (b)

Figure 3. Examples of z-knot fullerenes. (a) The smallest z-knot fullerene, isomer 34:1 (C_2). The unique zigzag vector is $(102_{17,34})$, with self-intersections of type I on one-third of the edges of the polyhedron (marked by thick lines in the Schlegel diagram). These 17 edges are disjoint and hence span a perfect matching (Kekulé structure) on the fullerene. 34:1 is not only the smallest z-knot fullerene, but the smallest *minimal* z-knot fullerene. Dotted curves indicate lines of latitude of the Föppl structure[29] of the vertices. (b) A z-knot fullerene, 40:22 (C_1), with z-vector $(120_{21,39})$. Thick lines mark the 21 edges of type I; dotted curves denote lines of latitude. This is the smallest *near-Kekulé* z-knot fullerene.

knot, *z-knot fullerenes* (with obvious extension to other trivalent polyhedra). Clearly, the dual of a z-knot fullerene is itself a z-knotted polyhedron, and both the z-knot fullerene and its dual are z-uniform, z-transitive, and z-balanced.

The smallest z-knot fullerene (isomer 34:1) and another small z-knot fullerene (40:22), the only z-knot fullerene on 40 vertices, are illustrated in Figure 3. Both are smallest examples of z-knot fullerenes with respect to minimality properties related to Kekulé structures derived from their unique zigzag circuits (section 7).

In passing, it can be noted that the knots whose projections appear for z-knot fullerenes are all nontrivial, i.e., are not disguised presentations of the simple circuit. This observation follows from the algorithm for reducing a presentation of an alternating knot to a simple form: unfold every one of the vertices that disconnect it, until we obtain a 2-connected 4-valent graph; if this 2-connected graph is not a simple circuit, then the alternating knot is nontrivial, by application of the Jones polynomial.[7] As all fullerenes are 3-connected, and since vertex-connectivity implies edge-connectivity, it is impossible to reduce their z-knots in this way, and all fullerene z-knots are therefore nontrivial.

Tables 6−8 give the statistics of z-knot polyhedra in small trivalent polyhedra, general fullerenes, and isolated fullerenes. Table 6 shows that, in the range studied, the number of z-knot trivalent polyhedra is increasing for $n \geq 10$, and an increasing proportion of the z-knot polyhedra have only trivial C_1 symmetry. The proportion of polyhedra that are knots starts to decrease from $n = 20$. By $n = 24$, 34% of the polyhedra are z-knots, and 99% of those z-knots have C_1 symmetry. For $n \leq 24$, minimal knots are found only for $n \equiv 2$ (mod 4) and, though increasing in number, still account for less than 1% of the z-knots on 22 vertices.

The tabulation of z-knot general fullerenes (Table 7) shows some similar patterns. In the range studied, the number of z-knots shows an odd−even effect between $n \equiv 0$ (mod 4) and $n \equiv 2$ (mod 4), each subseries increasing from $n \geq 40$, the number of minimal fullerenes increasing more strongly for $n \equiv 2$ (mod 4). The z-knots are predominantly of C_1 symmetry, and, in the range, z-knots of C_2 symmetry occur only for $n \equiv 2$ (mod 4), where the number of edges of the fullerene is odd, and, since e_1 is found to be odd for all z-knot fullerenes (see (3) below), this is consistent with a structure in which the C_2 axis passes through one edge of type I and one hexagon center.

Table 6. Statistics of Occurrence of Knots in Small Trivalent Polyhedra (Equivalently, Planar Triangulations) on n Vertices[a]

n	N_P	N_{knot}	N_{min}	symmetries
4	1	0	0	
6	1	1	1	$D_{3h}(1)$
8	2	0	0	
10	5	3	1	$C_{2v}(1)$,$C_{3v}(1)$,$D_{5h}(1)$
12	14	4	0	$C_1(2)$,$C_s(2)$
14	50	22	4	$C_1(8)$,$C_2(3)$,$C_{2v}(4)$,$C_s(6)$,$D_{7h}(1)$
16	233	70	0	$C_1(53)$,$C_s(15)$,$C_{3v}(2)$
18	1249	482	13	$C_1(398)$,$C_s(45)$,$C_2(27)$,$C_{2v}(10)$,$D_{3h}(1)$, $D_{9h}(1)$
20	7595	2955	0	$C_1(2816)$,$C_s(138)$,$C_3(1)$
22	49566	17901	168	$C_1(17306)$,$C_s(366)$,$C_2(196)$,$C_3(5)$, $C_{2v}(33)$,$D_{11h}(1)$
24	339722	114642	0	$C_1(113604)$,$C_s(1026)$,$C_{3v}(8)$,$C_3(4)$

[a] At each n, N_P is the total number of nonisomorphic polyhedra, N_{knot} is the total number of knot polyhedra, and N_{min} is the number that are minimal knots (knots where every vertex is incident to exactly one edge of type I). A breakdown of the z-knots by symmetry is given in the final column.

Table 7. Statistics on All z-Knot Fullerenes C_n with $n \leq 74$ Vertices[a]

n	N_{full}	N_{knot}	N_{min}	$N(C_1)$	$N(C_2)$	$N(C_3)$	$N(D_3)$
34	6	1	1	0	1	0	0
36	15	0	0	0	0	0	0
38	17	4	1	1	2	0	1
40	40	1	1	1	0	0	0
42	49	6	2	2	3	0	1
44	89	9	6	9	0	0	0
46	116	15	2	6	9	0	0
48	199	23	13	23	0	0	0
50	271	30	6	21	8	0	1
52	437	42	13	42	0	0	0
54	580	93	16	69	23	0	1
56	924	87	26	87	0	0	0
58	1205	186	11	155	30	1	0
60	1812	206	63	206	0	0	0
62	2385	341	20	297	41	2	1
64	3465	437	148	436	0	1	0
66	4478	567	64	507	59	0	1
68	6332	894	203	892	0	2	0
70	8149	1048	139	967	80	1	0
72	11190	1613	255	1612	0	1	0
74	14246	1970	200	1865	104	0	1

[a] For each value of n, N_{knot} is the total number of z-knot fullerenes, N_{min} is the number of minimal z-knot fullerenes (where every vertex is incident to exactly one edge of type I), and N_G is the number of z-knot fullerenes with point group symmetry G. Note that $N_{knot} = 0$ for all fullerenes with $n \leq 32$. The group D_5 appears first as the point group of a z-knot fullerene at 90 vertices.

As Table 8 shows, z-knot fullerenes account for only 19 out of a total of 2706 isolated-pentagon fullerenes with $n \leq 100$, and of these 19 only 7 are Kekulé knots, occurring at 86, 94, and 98 vertices (Table 8).

We now make the following very general conjecture about e_1:

$$e_1 \text{ for any } z\text{-knotted trivalent plane graph is odd} \quad (3)$$

This conjecture is supported by extensive computations. For

Table 8. Isolated-Pentagon *z*-Knot Fullerenes C_n with $n \leq 100$ Vertices[a]

n	signature		Kekulé?
86	43, 86	C_2:2	yes
90	47, 88	C_1:7	no
	53, 82	C_2:19	no
	71, 64	C_2:6	no
94	47, 94	C_1:60; C_2:26, C_2:126	yes
	65, 76	C_2:121	no
	69, 72	C_2:7	no
96	49, 95	C_1:65	near
	53, 91	C_1:7, C_1:37, C_1:63	no
98	49, 98	C_2:191, C_2:194, C_2:196	yes
	63, 84	C_1:49	no
	75, 72	C_1:29	no
	77, 70	C_1:5; C_2:221	no
100	51, 99	C_1:371, C_1:377, C_3:221	near
	53, 97	C_1:29, C_1:113, C_1:236	no
	55, 95	C_1:165	no
	57, 93	C_1:21	no
	61, 89	C_1:225	no
	65, 85	C_1:31, C_1:234	no

[a] For each vertex number n and signature (i.e. the pair of numbers e_1, e_2), the *z*-knot fullerenes are listed by symmetry and position in the spiral lexicographic order.[6] Kekulé *z*-knot fullerenes are those with $e_1 = n/2$; near-Kekulé are those with $e_1 = n/2 + 1$. No isolated-pentagon *z*-knot fullerenes are found for $n \leq 84$.

example, e_1 is found to be odd for all *z*-knotted cubic polyhedra ($n \leq 24$), all *z*-knot fullerenes C_n ($n \leq 74$), and all isolated-pentagon *z*-knot fullerenes C_n ($n \leq 120$), a total of over 140 000 *z*-knots. The condition of trivalence is a necessary restriction in this conjecture, as, for example, the dual of the $(2k + 1)$-gonal prism has $e_1 = 4k + 2$, as mentioned earlier and illustrated for $k = 1$ in Figure 1(c).

6. SYMMETRIES OF Z-KNOT FULLERENES

The symmetry groups describing fullerenes are limited in number: a fullerene may have (maximal) point group symmetry drawn from a list of 28 possibilities:[6,22] I_h, I, T_h, T_d, T, D_{6h}, D_{6d}, D_6, D_{5h}, D_{5d}, D_5, D_{3h}, D_{3d}, D_3, D_{2h}, D_{2d}, D_2, S_6, S_4, C_{3h}, C_{2h}, C_{3v}, C_3, C_{2v}, C_2, C_s, C_i, C_1. Fullerenes of low symmetry are predominant at large n, but examples for all of the possible groups appear early in the set (I is the last to appear, at 140 vertices). Inspection of the computational results for *z*-knot fullerenes in Tables 7 and 8 suggests that the symmetries of knot fullerenes are drawn from a much smaller list of possibilities. In a search that includes all fullerenes with $n \leq 100$ and all isolated-pentagon fullerenes with $n \leq 120$, only groups C_1, C_2, C_3, D_3, and D_5 are encountered. Smallest cases for four of these groups are given in Table 7, and the smallest D_5 *z*-knot fullerene is 90:99130, the unique D_5 fullerene with 90 vertices. Trivial symmetry appears to dominate; indeed for $n = 4m < 64$, all *z*-knot fullerenes have C_1 symmetry. Notably, all *z*-knot fullerenes found in our study are chiral.

Symmetry can be assigned not only to the underlying fullerene but also to the knot projection formed by its single, self-intersecting zigzag. Mark all edges of type I with one color, all edges of type II with another. Now, the zigzag must transform into itself (up to reversal of all arrows) under all symmetry operations belonging to the point group, G, of the underlying fullerene, as otherwise it would not be unique. Thus the set of e_1 edges of type I must comprise a whole number of orbits of G, as must the set of e_2 edges of type II. Recall that, in a spherical polyhedron, the site symmetry of an edge is C_{2v} or one of its subgroups C_2, C_s, or C_1. The orbits that may occur in the edge sets are therefore limited to sizes $|G|/4$, $|G|/2$, or $|G|/1$, though not all edge site groups occur for every fullerene group; site groups C_2 and C_s are mutually exclusive, for example.

We now use the conjecture (3) that e_1 is odd for all knot fullerenes. If e_1 is odd, then the set of edges of type I must be spanned by an odd number of orbits of odd size. Oddness of e_1 rules out all fullerene groups where the edge-compatible orbits are all even. In particular, centrosymmetric groups are not possible for *z*-knot fullerenes with odd e_1, since the inversion operation pairs the edges of a spherical polyhedron. Application of the orbit-parity argument to the grand list of 28 fullerene point groups reduces it to a minilist of 11 candidates for *z*-knot fullerene groups:

$$D_{5h}, D_5, D_{3h}, D_3, C_{3h}, C_{3v}, C_3, C_{2v}, C_2, C_s, C_1 \quad (4)$$

All five pure rotation groups in the minilist have been found as point groups of some *z*-knot fullerene. In contrast, the others, all groups that contain at least one mirror plane, have not been found. It is tempting to conjecture that all *z*-knot fullerenes are chiral and that the set

$$D_5, D_3, C_3, C_2, C_1 \quad (5)$$

is the complete list of point groups available to *z*-knot fullerenes. It is interesting that there is no such restriction to chiral symmetries for more general trivalent polyhedra: the $(2k + 1)$-gonal prisms have $D_{(2k+1)h}$ symmetry and are all *z*-knots; there are many *z*-knots of C_s symmetry in the series of bipartite trivalent polyhedra that have six square faces and all other faces hexagonal.[23]

7. KNOTS AND KEKULÉ STRUCTURES

A useful though not infallible indicator of stability of a π framework is that the system should possess a large number of Kekulé structures (KS). Every fullerene has at least three[24] and typically very many more; icosahedral C_{60} has 12 500[25] KS and is surpassed in this by 20 of its fullerene isomers.[26] An interesting feature of the definition of a knot-fullerene is that, in some special cases, a particularly simple Kekulé structure can be derived from the knot. The key to the connection is that we will be able in these cases to associate a formal double bond of a Kekulé structure with each edge of type I in the *z*-knot fullerene.

Consider an n-vertex trivalent plane graph G that is also a projection of a knot, i.e., has *z*-vector $((3n)_{e1,e2})$. It is easy to see (Figure 4) that (i) every vertex is incident to an even number of edges of type II, and (ii) every face is incident to an even number of edges of type I.

The proof of both statements is straightforward. Since G is *z*-knotted, one can choose an orientation in which edges of type I carry two opposite arrows and edges of type II carry two arrows in the same direction. By a Kirchhoff-like argument based on incoming and outgoing arrows, it can be seen that the vertices of a knotted trivalent graph then fall into two classes: n_1 vertices belong to class 1, where all three incident edges are of type I, and $n_2 = n - n_1$ vertices belong to class 2, where only one incident edge is of type I.

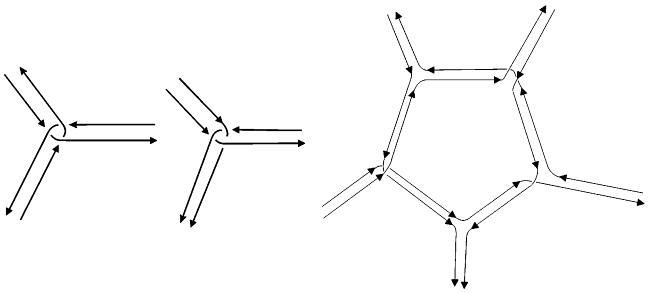

Figure 4. Pictorial proof by a Kirchoff-like argument that every vertex of a z-knot fullerene is incident to an even number of edges of type II, and, by duality, every face to an even number of edges of type I.

Thus, at each vertex, the number of incident edges of type I is odd, and the number of incident edges of type II is even. So, (i) is proved. Furthermore, as the dual graph has a zigzag structure in which e_1 and e_2 are exchanged, application of the same reasoning to the vertices of the dual shows that in a trivalent knotted graph every face contains an even number of type I edges. So, (ii) is also proved.

An association with Kekulé structures follows by counting edges and vertices. We have

$$2e_1 = 3n_1 + n_2 = 2n_1 + n \tag{6}$$

and

$$2e_2 = 2n_2 = 2n - 2n_1 \tag{7}$$

and hence

$$e_1 \geq n/2 \tag{8}$$

with the equality being achieved only for $n_1 = 0$. In other words, $e_1 = n/2$ when the edges of type I are disjoint ($n_1 = 0$) and span all vertices ($n = 2e_1$) and so form a perfect matching (Kekulé structure). G has signature $((3n)_{n/2,n})$.

We consider now more closely the case of z-knot fullerenes for which every vertex is incident to exactly one edge of type I, i.e., for which the number of edges of type I is equal to the minimal $n/2$. By extension, we will term such graphs *minimal* z-knots. Granted the conjecture (3) on e_1, the number of edges of type I of a z-knotted graph is odd, and hence the number of vertices in a minimal z-knot fullerene is doubly odd, i.e., $n \equiv 2 \pmod 4$.

By (ii) above, we know that every face contains an even number of edges of type I. As the faces of a fullerene are all pentagons or hexagons, and as the edges of type I are disjoint, it follows that every face of a z-knot fullerene is incident to zero or two edges of type I. In fact, since the argument depends on the independence number of the cycle of edges that constitute a face, it applies equally well to all z-knotted trivalent plane graphs in which no face is of size larger than 7; in all such graphs every face is incident to 0 or 2 edges of type I. Generalized fullerenes with face sizes 4, 5, and 6 or 5, 6, and 7 have been considered as competitive in stability with the classical 5, 6 fullerenes in some size ranges.[27,28]

Furthermore, exactly two faces of the minimal z-knot fullerene (or of the z-knotted trivalent plane graph with no face of size larger than 7) contain no edges of type I, and all other faces contain two edges of type I. This follows by counting: the number of faces of a fullerene trivalent polyhedron with n vertices is $n/2 + 2$, and, denoting by p_0, p_2 the numbers of faces containing respectively zero and two edges of type I

$$n/2 + 2 = p_2 + p_0 \tag{9}$$

and counting edges

$$2p_2 + 0p_0 = 2e_1 = n \tag{10}$$

with unique solution $p_2 = n/2$, $p_0 = 2$.

The two faces without edges of type I define uniquely the set of edges of type I over the whole fullerene. (Proof: Take one face F_0 with zero edges of type I. This face is adjacent to a set of faces, say, F_1, ..., F_p. Every pair F_i, F_{i+1} is incident to one edge, say e_i, that must be of type I since e_i is incident to one vertex of F_0. The face F_i is incident to edges e_i and e_{i-1} and so, all other edges of F_i are of type II. By induction, one is able to assign a type to every edge.)

An immediate consequence of the construction is that the two empty faces of the minimal knot are antipodal, in the sense that they span a diameter in the dual. Their centers can be taken as poles of the (in general distorted) sphere on which the fullerene is embedded. Making the equivalence between type I edges with formal double bonds of a carbon cage, it can be seen that a minimal z-knot fullerene defines a characteristic Kekulé structure: the North and South poles are the centers of the two faces devoid of double bonds, the remaining single bonds form latitudinal circuits and all double bonds lie on lines of longitude. The lantern-like structure with horizontal single bonds separated by vertical double-bond struts is reminiscent of the Föppl presentation of polyhedra:[29,30] in this case the polyhedron is a stack of circuits of vertices, without a vertex at either pole. The fullerene 34:1 in Figure 3(a) is an example of a fullerene polyhedron of this type.

An observation, though not a proven result, is that in all minimal-z-knot fullerenes found so far the two faces that are empty of type I edges are either both hexagons or both pentagons but never a pentagon/hexagon pair.

Chemically, this special Kekulé structure is not, of itself, indicative of special stability, as by definition it excludes benzenoid hexagons. Kekulé structures of this type, i.e., with lantern-like organization of single and double bonds, are not limited to z-knot fullerenes; icosahedral C_{20} and C_{60} have them, for example, without any association with knots or zigzags.

Minimal knots, as defined above, have $n/2$ edges of type I and are in complete correspondence with a Kekulé structure based on a decoration of the edges in a Föppl presentation. A similar near-Kekulé construction can be found for knots that are near-minimal. We have so far called a trivalent graph *minimal* if it is z-knotted with $e_1 = n/2$ and $n \equiv 2 \pmod 4$. z-knotted graphs with $n \equiv 0 \pmod 4$ cannot have $e_1 = n/2$ but may reach $e_1 = n/2 + 1$, which if conjecture (3) holds, is the minimum value of e for a graph of this vertex count. By (3), when $e_1 = n/2 + 1$, $n_1 = 1$ and so there is exactly one vertex from which three edges of type I emanate. Solving (9) and (10) with $2e = n + n_1 = n + 1$ gives $p_0 = 1$ and $p_2 = n + 1$, showing that exactly one face is empty of edges of type I, and all others contain exactly two edges of type I. The unique empty face (which may be either a hexagon or a pentagon in different cases) and the distinguished vertex are again antipodal, by construction.

Figure 3(b) shows an example of such a fullerene. The edges of type I cannot in this case correspond to a perfect matching, since $e_1 \neq n/2$. However, their distribution differs only at one pole of the Föppl arrangement, which for these near-Kekulé knots has a vertex at one pole and the center of a face at the other. Three edges of type I radiate from the pole vertex, and the face at the antipode is empty of type-I edges. A Kekulé structure can be formally recovered by imagining the pole vertex to be truncated, to give an empty triangular face, from which double bonds radiate, and an enlargement of the three bordering faces by one edge.

The conjecture (3) that e_1 is odd for trivalent knotted graphs implies that the equality cannot be reached when $n/2$ is even. We will call a z-knot trivalent graph a Kekulé graph if it has

$$e_1 = n/2;\ n \equiv 2 \pmod 4); \quad n_1 = 0 \tag{11}$$

and a near-Kekulé graph if it has

$$e_1 = n/2 + 1;\ n \equiv 0 \pmod 4); \quad n_1 = 1 \tag{12}$$

8. RAILROADS AND KNOTS

A *railroad* in a fullerene is a circuit of hexagonal faces (called *simple* if it is not self-intersecting) such that each hexagon is adjacent to its two neighbors on *opposite* sides. Simple railroads are also called *straight zones*.[31] To each railroad is associated a pair of boundary zigzags, which are parallel (in the sense of disjoint) if the railroad is simple, but which intersect if the railroad has self-intersection(s). Fullerenes that have no railroads, simple or otherwise, are called *tight*, as in a sense the pentagons of the fullerene are then pulled as tightly together as possible in such a case.[13] The z-knot fullerenes are of course all tight by definition. We conjecture on the basis of calculations on fullerenes with $n \leq 74$ (general) and $n \leq 120$ (isolated-pentagon) that there is at least one tight fullerene at every vertex count $n \geq 20$, $n \neq 22$.

It is easy to check the following three statements about railroads.

(i) Any simple zigzag circuit separates the 12 pentagons of the fullerene into six that are "internal" and six that are "external" to the circuit. On the spherical surface, any two disjoint zigzags can thus be seen as concentric. This is the simplest case of a local Euler formula that expresses the number of pentagons enclosed by a curve in terms of the balance of in- and out-pointing free valences of the vertices on the curve.[22] The so-called zigzag[32] nanotubes consist precisely of stacks of simple railroads, which may be topped and tailed by two hemispherical caps. Insertion of extra, parallel zigzags between the railroads generates an infinite series of tubular fullerenes with the same caps.

(ii) A fullerene has a simple railroad if and only if it has at least two disjoint simple zigzags. If there is a simple railroad, then there are two disjoint simple zigzags, by definition. If there are two disjoint simple zigzags, then, as each separates the 12 pentagons into two sets of 6, a simple railroad must exist between the two zigzags. The smallest icosahedral fullerene with a simple railroad has 80 vertices; this fullerene (80:7) has 6 such railroads, each of length 10, each railroad circumscribing a motif comprising a pentagon and its first and second neighbors, i.e., running around an equator of the polyhedron; every pair of railroads intersects in two hexagons; each hexagon is at the intersection of two railroads (Figure 5).

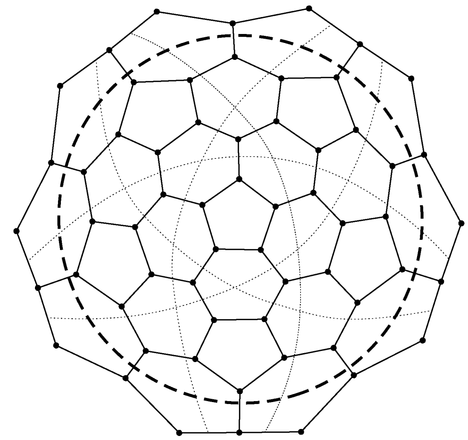

Figure 5. Railroad structure in icosahedral C_{80}. A simple railroad (dashed circle) runs through 10 hexagons around each cap of six pentagons; each such railroad is intersected in all pairs of opposite hexagons by railroad from the same orbit, centered on the second-neighbor pentagons of the icosahedral arrangment. Railroads centered on antipodal pentagons do not intersect.

(iii) If a fullerene has no railroads, then the number of zigzags is at most 30, as each zigzag must be adjacent to at least one pentagon on the right and at least one on the left, and each such contact involves two pentagon sides. For example, C_{140} has z-vector (28^{15}). In fact, in computations on several hundred thousand fullerenes, we have not encountered more than 15 zigzags in any tight fullerene, and it seems reasonable to conjecture that 15 is the true upper bound to the number of zigzags in such fullerenes.

To each railroad, we can associate a closed curve, constructed, for example, by connecting the centers of neighboring railroad hexagons through the midpoints of opposite edges. This curve may be simple (without self-intersection), or it may admit self-intersection. Points of intersection can be double, where the curve passes twice through a given hexagon, or triple, where it passes through three times. The smallest fullerene to exhibit a simple railroad is 30:1 (D_{3h}) with an equatorial band of five hexagons. A fullerene with a triple intersection is illustrated in Figure 6. Figure 7(a) shows the smallest general fullerene (50:13) to exhibit a double self-intersection of a railroad, and Figure 8(a) shows the smallest isolated-pentagon fullerene of this type (96:187, obtained by application of the "quadrupling" or "chamfering" operation[33] to the unique fullerene of 24 vertices).

Railroads without triple self-intersection can be seen as projections of alternating knots, and every fullerene with simple or doubly intersecting railroads has therefore an associated list of knots. This is a second context in which knots and fullerenes appear together: we have seen that a fullerene itself may be a zigzag knot, and now we see that the railroads of a fullerene may yield knots. The two situations are mutually exclusive in that the first requires the fullerene to have only one zigzag, the second to have at least two. Each simple railroad is just a minimal projection of the trivial knot, but self-intersecting railroads can also

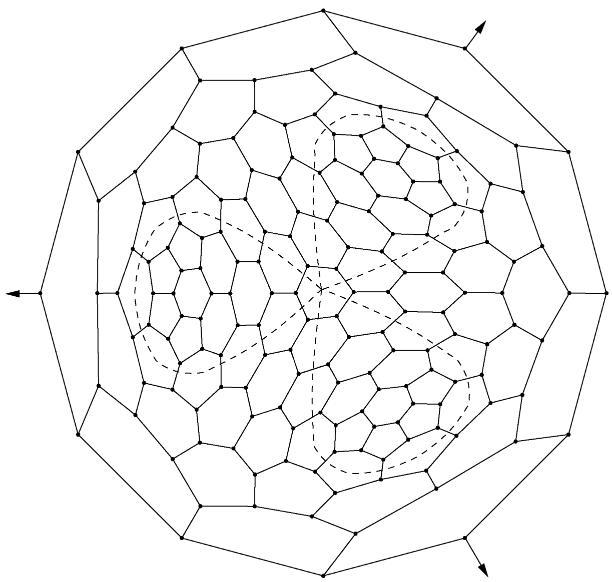

Figure 6. A case of a railroad with triple self-intersections.[13] The fullerene illustrated here has 176 vertices and is of C_{3v} symmetry.

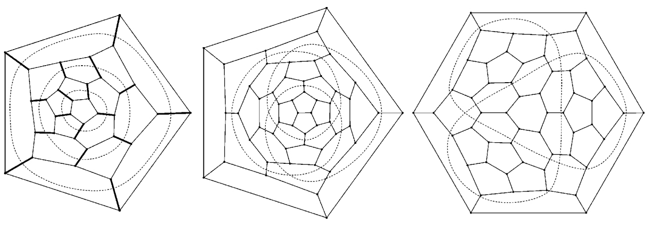

(a) (b) (c)

Figure 7. General fullerenes with self-intersecting railroads. Railroads are indicated by dashed lines on the Schlegel diagram. (a) The smallest fullerene with self-intersection of railroads, 50:13 (C_{2v}), has a railroad that is a nonminimal projection of the trivial knot; (b) 52:94 (D_{2d}) is the smallest fullerene with a self-intersecting railroad that is a projection of a nontrivial knot (in this case the figure-of-eight or Flemish knot). This fullerene isomer is also the smallest example of a fullerene that is not *z*-balanced; (c) 54:119 (D_{3h}) is the smallest fullerene that corresponds to a trefoil knot.

give this knot in a realization from which the crossing can be removed by simple untwisting; if the railroad has no loops, the projection is minimal. In fact 50:13 in Figure 7(a) shows a nonminimal projection of the trivial knot. More interesting are the cases in which nontrivial knots appear. We may call a fullerene that contains a railroad corresponding to a nontrivial knot, an *r-knot* fullerene.

Cases of self-intersecting railroads are listed in Table 9 for general fullerenes with $n \leq 60$ vertices and in Table 10 for isolated-pentagon fullerenes with $n \leq 114$ vertices. In these ranges of n, triple intersection of a railroad is not found, and so all the tabulated fullerenes are projections of alternating knots. The tables give data on the *z*-vector and the knots associated with the railroad(s). It can be seen that many are simply disguised trivial knots, 0_1, but a variety of well-known knots also appear. 52:94 and 54:119 are *r*-knot fullerenes. Figure 7 shows the smallest fullerenes in which the knots 0_1, 3_1, and 4_1 appear as a consequence of self-intersection of railroads. The smallest isolated-pentagon fullerenes to yield projections of three of the more complicated knots are shown in Figure 8.

Figure 9 shows projections of the six different knots found in the range. 3_1 is the trefoil or overhand knot, and 4_1 is the figure-of-eight knot, also known as the Flemish or Savoy knot. Trefoil fullerenes with isolated pentagons are not found in the investigated range (Table 10), but Flemish *r*-knot fullerenes with isolated-pentagons do occur (114:1738 and 114:3419). Examples of isolated-pentagon *r*-knot fullerenes corresponding to three more complicated knots also appear in the tabulated range. These are all knots that have Conway graphs[21] as projections.

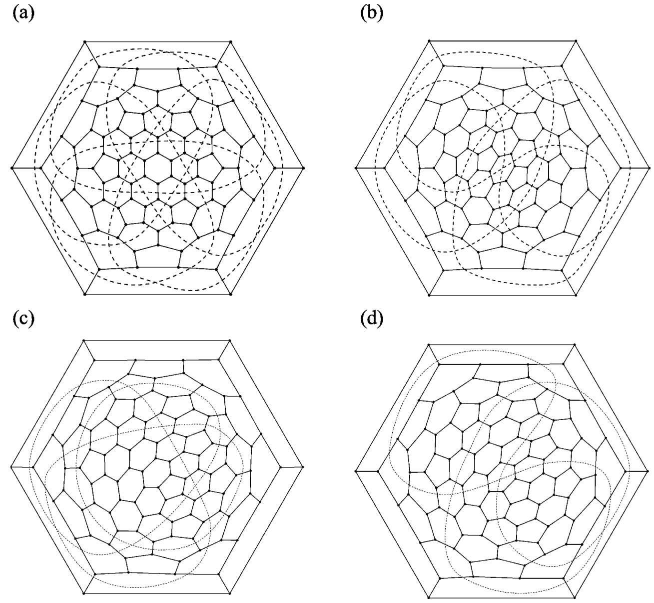

Figure 8. Isolated-pentagon fullerenes with self-intersecting railroads (indicated by dashed lines). (a) The smallest isolated-pentagon fullerene with self-intersection of railroads, 96:187 (D_{6d}), has a railroad that is a projection of the Conway-graph knot $(4 \times 6)^*$. The two polar hexagons are not involved in the railroad, but every other hexagon is traversed twice, leading to 24 self-intersections of the railroad. (b) 104:823 (D_{3h}) is the smallest isolated pentagon fullerene with a railroad that is a projection of the knot 9_{40} ((3×3) in the Conway graph notation). This fullerene also supports three simple railroads of length 12, so that its railroad set is a projection of a four-component link. Apart from three equatorial hexagons, each hexagon is traversed either twice by the knot railroad or once each by two distinct railroads. (c),(d) The fullerene 112:3341 has railroads that correspond to projections of two nontrivial knots: the figure-of-eight or Flemish knot (c) and the knot $8_{18} \equiv (2 \times 4)^*$ (d).

Table 9. Fullerenes C_n ($n \leq 60$) Having Self-Intersecting Railroads[a]

isomer	group	orbits	*z*-vector	knots
50:13	C_{2v}	2,1,1	$20; \mathbf{24}^2_{0,1}, 82_{14,5}$	0_1
52:94	D_{2d}	2,2	$38^2_{0,3}, \mathbf{40}^2_{0,4}$	4_1
54:13	C_2	2,2,1,1	$20^3; \mathbf{24}^2_{0,1}, 54_{2,5}$	0_1
54:119	D_{3h}	3,2,1	$16^3; \mathbf{36}^2_{3,0}, 42_{0,3}$	3_1
60:27	C_s	1,1,1,1	$14; \mathbf{26}^2_{0,1}, 114_{18,14}$	0_1
60:34	C_s	1,1,1	$\mathbf{26}^2_{0,1}, 128_{19,23}\mathrm{z}$	0_1
60:207	C_s	1,1,1	$\mathbf{28}^2_{0,1}, 124_{17,21}$	0_1
60:208	C_{2v}	2,1,1	$\mathbf{28}^2_{0,1}, 60_{0,8}, 64_{8,2}$	0_1
60:1379	C_{2v}	2,2	$\mathbf{28}^2_{0,1}, 62^2_{2,6}$	0_1

[a] For each fullerene, listed by symmetry and position in the spiral lexicographic order,[6] the zigzag vector *z* is given, together with the sizes of the orbits of zigzags and the list of railroad knots. A bold entry in a *z*-vector shows the origin of a significant knotted railroad. For completeness the trivial knots arising from simple railroads (if any) are also listed, with multiplicity, in brackets. Knots are named in the Rolfsen notation[19,21] and illustrated in Figure 9.

Table 10. Isolated-Pentagon Fullerenes C_n ($n \leq 114$) Having Self-Intersecting Railroads[a]

isomer	group	orbits	*z*-vector	knots
96:187	D_{6d}	2,2	24^2; $\mathbf{120}^2_{12,12}$	(0_1); $(4 \times 6)^*$
104:823	D_{3h}	3,3,2	24^6; $\mathbf{84}^2_{0,9}$	$(0_1)^3$; $9_{40} \equiv (3 \times 3)^*$
106:624	C_{3v}	3,1,1	$50^3_{0,1}$, $\mathbf{84}^2_{0,9}$	$9_{40} \equiv (3 \times 3)^*$
108:897	D_{3h}	6,2	26^6; $\mathbf{84}^2_{0,9}$	$9_{40} \equiv (3 \times 3)^*$
112:3341	D_2	2,2,2	24^2; $\mathbf{64}^2_{0,4}$, $80^2_{0,8}$	4_1, $8_{18} \equiv (2 \times 4)^*$
114:9	C_{2v}	2,2,1	$\mathbf{40}^2_{0,1}$, $86^2_{2,6}$, $90_{3,6}$	0_1
114:1738	C_1	1,1,1,1,1	$50_{0,1}$, $\mathbf{64}^2_{0,4}$, $82_{0,8}$, $82_{1,7}$	4_1
114:2338	C_{2v}	1,1,1,1	$42_{0,1}$, $\mathbf{80}^2_{0,8}$, $140_{14,12}$	$8_{18} \equiv (2 \times 4)^*$
114:3419	C_2	1,1,1	$\mathbf{64}^2_{0,4}$, $214_{13,46}$	4_1

[a] Conventions as in Table 9. Where the Rolfsen notation is not available, the Conway-graph notation[21] is used for the alternating knot corresponding to the railroad. All knots are illustrated in Figure 9.

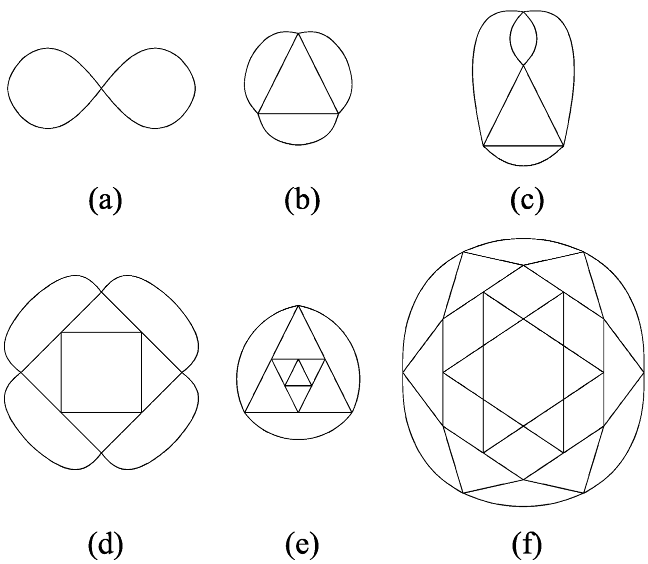

Figure 9. Knots that appear in fullerenes with self-intersecting railroads. (a)−(c) The top row shows the three knots (including the trivial knot 0_1 in a nonminimal projection) that appear for fullerenes with $n \leq 60$ vertices: 0_1, 3_1, and $4_1 = (2 \times 2)^*$. (d)−(f) The bottom row shows the first three Conway-graph knots that appear for isolated-pentagon fullerenes: $8_{18} \equiv (2 \times 4)^*$, $9_{40} \equiv (3 \times 3)^*$, and $(4 \times 6)^*$.

The Conway graph $(k \times m)^\star$ is a generalization of the antiprism with two m-gonal, $2m$ triangular, and $(k - 2)m$ quadrangular faces, constructed from a single m-cycle by successively inscribing a further $k - 1$ m-gons, the vertices of each new m-gon being the edge midpoints of its predecessor, finally adding m edges to link the consecutive vertices of the original cycle. The point group of the graph $(k \times m)^\star$ is D_{mh} for k even, and D_{md} for k odd, apart from the small cases $(2 \times 3)^\star$ and $(3 \times 4)^\star$ where it is O_h. In this notation, $(2 \times 3)^\star$ is the octahedron, $(3 \times 4)^\star$ is the cuboctahedron, and $(2 \times m)^\star$ is the m-gonal antiprism. The three Conway graphs relevant to Table 10 are shown in Figure 9. More complex knots will be encountered for larger numbers of vertices; Figure 10 shows three striking symmetrical knots that appear among the isomers of C_{120}, for example.

The projection of a railroad curve is itself a plane graph. It can be shown, using arguments following from local Euler formulas for the regions enclosed by the curve,[13] i.e., the faces of the graph, that no curve for which there would be a face of size six or more can correspond to a railroad. It would be interesting to know necessary and sufficient conditions for those curves that can occur for railroads in a fullerene.

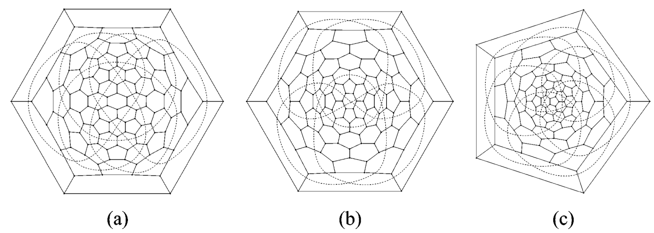

Figure 10. Three symmetric railroad knots in isolated-pentagon isomers of C_{120}. Self-intersecting railroads in (a) 120:10678, (b) 120:10733, and (c) 120:766.

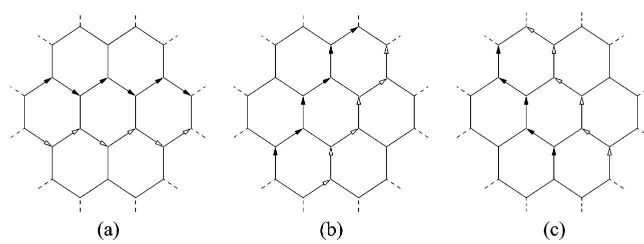

Figure 11. The three parallel classes of zigzag in the graphite sheet. In graphite, all are infinite and simple i.e., without self-intersection, and fall into a single orbit. In achiral nanotubes, one of the classes becomes an infinite set of parallel finite zigzags, the others remain infinite; in chiral nanotubes, all three remain infinite (see text).

9. CONCLUSION

Finally, it should be noted that the zigzag/railroad formalism is also applicable to infinite graphs, for example, the open nanotubes and the graphite sheet, where both zigzags and railroads can become doubly infinite rays (which can be seen as circuits including the point at infinity). The graphite sheet has three parallel classes of infinite railroads, each of them simple; accordingly it has three parallel classes of infinite simple zigzags (Figure 11) that form a single orbit. Graphite is therefore a *z*-transitive graph. Nanotubes are formally constructed by rolling up the graphite sheet, with each tube identified by a two-parameter lattice vector, and their zigzag structure derives from that of graphite itself. The three types of nanotube, zigzag, armchair, and chiral,[32] have parameter signatures $(n, 0)$, (n, n), (n, m) $(n \neq m)$. Zigzag structures of these three types are as follows: (a) For $(n, 0)$: two orbits of simple zigzags, one composed of finite circuits of length $2n$, the other of doubly infinite rays. The first orbit consists of concentric circuits around the body of the tube, the second of two parallel classes related by reflection. (b)

For (n, n): two orbits of simple zigzags, both consisting of doubly infinite rays, one "vertical" and one "oblique". (c) For (n, m), $n \neq m$: three orbits of doubly infinite rays, each consisting of a parallel class of helically wound zigzags wrapping around the long axis of the tube.

In all three cases, all zigzag vectors of the nanotube are without self-intersection, and the stack within each parallel class of zigzags corresponds to a stack of doubly infinite railroads. Unlike graphite, the open ended infinite nanotube is not z-transitive.

The concept of the zigzag is not limited to fullerenes and spherical polyhedra. A similar analysis can be applied to the zigzags of polyhex tori, carbon networks on surfaces of higher genus such as in the plumber's nightmare carbon foams, and, the definition of left/right edges being local, to analogues of fullerenes on nonorientable surfaces, such as the Klein bottle and projective plane.[34] The analysis also extends to 3D crystals such as diamond.

Zigzag circuits and z-vectors give a different way of looking at polyhedral and related structures, complementing the more immediately apparent face and vertex information. Use of the computer to explore this hidden structure reveals a number of properties of fullerenes as a chemically interesting subset of trivalent polyhedra. Hidden in the zigzag structures of some fullerenes are complicated knots based on their zigzags, and hidden in some of their knots are specific Kekulé structures. Pairing of nonintersecting zigzags gives rise to hexagon-based railroad structures and the appearance of further complex and beautiful knots. It remains to be seen how these mathematical structures impinge on the chemical properties of fullerene isomers, but the z-vector already shows potential for chemical application through its connections with both electronic and combinatorial structure.

ACKNOWLEDGMENT

EU Research Training Networks HPRN-CT-2002-00177 and HPRN-CT-2001-00272, Algebraic Combinatorics in Europe, and BQR (ENS) are thanked for financial support and Com^{2}MaC (Postech, Korea) for hosting the workshop "Two-face embeddings of graphs, and applications" during which this paper was completed.

REFERENCES AND NOTES

(1) Barnette, D. *Map Coloring, Polyhedra, and the Four-Color Problem*; Dolciani Mathematical Expositions, American Mathematical Society: Providence, RI, 1983.
(2) Eberhard, V. *Zur Morphologie der Polyeder*; Leipzig, 1891.
(3) Grünbaum, B. *Convex Polytopes*; Wiley-Interscience: New York, 1967; p 276.
(4) Grünbaum, B.; Motzkin, T. S. The number of hexagons and the simplicity of geodesics on certain polyhedra. *Can. J. Math.* **1963**, *15*, 744−751.
(5) Balaban, A. T. Theoretical examination of electrically charged buckytubes. *Bull. Soc. Chim. Belges* **1996**, *105*, 383−389.
(6) Fowler, P. W.; Manolopoulos, D. E. *An Atlas of Fullerenes*; Oxford University Press: Oxford: 1995.
(7) Jablan, S. Geometry of Fullerenes. http://members.tripod.com/~modularity/ful.htm.
(8) New software used in this paper is described at http://www.liga.ens.fr/~dutour /plangraph.
(9) Brinkmann, G.; McKay, B. plantri program, http://cs.anu.edu.au/people/bdm/plantri.
(10) Rogers K. M.; Fowler, P.W. Spiral codes and Goldberg representations of icosahedral fullerenes and octahedral analogues. *J. Chem. Inf. Comput. Sci.* **2001**, *41*, 108−111.
(11) Coxeter, H. S. M. *Regular Polytopes*; Dover: New York, 1973.
(12) Shank, H. The theory of left-right paths. In *Combinatorial Mathematics III, Proceedings of 3rd Australian Conference, St. Lucia 1974*; Lecture Notes in Mathematics 452; Springer-Verlag: Berlin, 1975; pp 42−54.
(13) Deza, M.; Dutour, M. Zigzag structure of simple two-faced polyhedra. *Combinatorics, Probability Comput.* in press.
(14) Goldberg, M. A class of multi-symmetric polyhedra. *Tohoku Math. J.* **1937**, *43*, 104−108.
(15) Brinkmann, G.; Harmuth, T. Personal communication.
(16) Deza, M.; Huang, T.; Lih, K.-W. Central circuit coverings of octahedrites and medial polyhedra. *J. Math. Res. Exposition* **2002**, *22*, 49−65.
(17) Coxeter, H. S. M. Virus macromolecules and geodesic domes. In *A Spectrum of Mathematics*; Butcher, B. C., Ed.; Oxford University Press/Auckland University Press: Oxford/Auckland, 1971; pp 98−107.
(18) Deza, M.; Dutour, M.; Goldberg-Coxeter construction for 3- or 4-valent plane graphs. *Electron. J. Combinatorics* Submitted for publication.
(19) Rolfsen, D. *Knots and Links*; Publish or Perish Press: Wilmington, 1976.
(20) Likorish, W. B. R. *An Introduction To Knot Theory*; Springer-Verlag: New York, 1997.
(21) Kawauchi, A. *A Survey of Knot Theory*; Birkhäuser, Basel, 1996.
(22) Fowler, P. W.; Manolopoulos, D. E.; Redmond, D. B.; Ryan, R. Possible symmetries of fullerene structures. *Chem. Phys. Lett.* **1993**, *202*, 371−378.
(23) Deza, M.; Dutour, M. *Two-faced Planar Maps.* Book in preparation.
(24) Klein, D. J.; Liu, X. Theorems for carbon cages. *J. Math. Chem.* **1992**, *11*, 199−205.
(25) Kroto, H. W.; Heath, J. R.; Curl, R. F.; Smalley, R. E. C_{60}: Buckminsterfullerene *Nature* **1985**, *318*, 162−163.
(26) Austin, S. J.; Fowler, P. W.; Hansen, P.; Manolopoulos, D. E.; Zheng, M. Fullerene isomers of C_{60}: Kekulé counts versus stability. *Chem. Phys. Lett.* **1994**, *228*, 478−484.
(27) Gao, Y.-D.; Herndon, W. C. Fullerenes with four-membered rings. *J. Am. Chem. Soc.* **1993**, *115*, 8459−8460.
(28) Ayuela, A.; Fowler, P. W.; Mitchell, D.; Schmidt, R.; Seifert G.; Zerbetto, F. C_{62}: theoretical evidence for a nonclassical fullerene with a heptagonal ring. *J. Phys. Chem.* **1996**, *100*, 15634−15636.
(29) Föppl, L. Stabile Anordnungen von Elektronen in Atom. *J. Reine Angew. Math.* **1912**, *141*, 251−301.
(30) Brown, L. D.; Lipscomb, W. N. Closo Boron Hydrides with 13 to 24 Boron Atoms. *Inorg. Chem.* **1977**, *16*, 2989−2996.
(31) Deza, M.; Fowler, P. W.; Shtogrin, M. Zones and zigzag structure in icosahedral fullerenes and icosadeltahedra. *J. Chem. Inf. Comput. Sci.* **2003**, *43*, 595−599.
(32) See e.g. Dresselhaus, M. S.; Dresselhaus, G.; Eklund, P. C. *Science of Fullerenes and Carbon Nanotubes*; Academic Press: New York, 1996.
(33) Fowler, P. W.; Cremona J. E.; Steer, J. I. Systematics of bonding in nonicosahedral carbon clusters. *Theor. Chim. Acta* **1988**, *73*, 1−26.
(34) Deza, M.; Fowler, P. W.; Rassat, A.; Rogers, K. M. Fullerenes as tilings of surfaces. *J. Chem. Inf. Comput. Sci.* **1996**, *40*, 550−558.

CI049955H